J|A|C|S
ARTICLES
Published on Web 03/29/2007

The Synthesis of Dichlorodiazirine and the Generation of Dichlorocarbene: Spectroscopy and Structure of Dichlorocarbene Ylides

Robert A. Moss,*,† Jingzhi Tian,† Ronald R. Sauers,† Daniel H. Ess,‡ Kendall N. Houk,‡ and Karsten Krogh-Jespersen*,†

Contribution from the Department of Chemistry and Chemical Biology, Rutgers, The State University of New Jersey, New Brunswick, New Jersey 08903, and Department of Chemistry and Biochemistry, University of California, Los Angeles, California 90095

Received December 5, 2006; E-mail: moss@rutchem.rutgers.edu; krogh@rutchem.rutgers.edu

Abstract: Reaction of 2,4-dinitrophenoxychlorodiazirine (**13**) with chloride ions affords dichlorodiazirine (**4**). Photolysis of **4** generates dichlorocarbene. In laser flash photolysis (LFP) experiments, CCl_2 forms chromophoric ylides or oxides with pyridine, 2-picoline, thioanisole, and oxygen. Spectroscopic and computational studies of the ylides are reported. The UV spectrum of CCl_2 in solution, however, is not observed. It appears possible that CCl_2 is rapidly captured by oxygen to afford a chromophoric dichlorocarbene carbonyl oxide. We present a theoretical analysis of this process.

Introduction

Hine's historic investigations of the hydrolysis of haloforms[1] and Doering's demonstration that the dehydrohalogenation of chloroform in the presence of an alkene gave a dihalocyclopropane[2] established dichlorocarbene (CCl_2) as an iconic representative of divalent carbon species. There are many thermal methods for the generation of CCl_2,[3] but few photochemical options that lend themselves to spectroscopic studies.

Over the years, several aromatic adducts of CCl_2 have been shown to extrude the carbene upon photolysis. Examples include the CCl_2 adducts of styrene,[4a] 1,4-dihydronaphthalene,[4b] indane,[4c] and phenanthrene (**1**).[5]

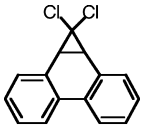

1

Unfortunately, photoextrusion of CCl_2 from these precursors necessarily leaves behind an equivalent of an aromatic byproduct, which can interfere with UV spectroscopic studies. In the specific case of precursor **1**, attempts to observe the UV spectrum of CCl_2 by laser flash photolysis (LFP) were inconclusive: any spectroscopic signature of the carbene was "overwhelmed" by absorptions of triplet phenanthrene.[5]

An imaginative approach to the spectroscopic study of CCl_2 was reported in 1967 by Milligan and Jacox,[6] who photolyzed cyanogen azide in chlorine-doped Ar matrices at 14 K, generating CCl_2 by the reaction of photochemically produced carbon atoms with Cl_2; cf. eq 1.

$$N_3CN \xrightarrow[-N_2]{h\nu} NCN \xrightarrow{h\nu} :C=N_2 \xrightarrow{-N_2} \text{“C”} \xrightarrow{Cl_2} :CCL_2 \quad (1)$$

Presumably, this reaction proceeded through cyanonitrene which photoisomerized to diazomethylene.[7] Nitrogen loss then gave carbon atoms which were captured by chlorine, yielding CCl_2. Electronic spectroscopy revealed "a weak band system appearing between 4400 and 5600 Å [...] attributed to CCl_2."[6] Confirmation of this assignment (revised to 4600−5300 Å) was later provided by photolysis of CD_2Cl_2 in an Ar matrix, where CCl_2 was again generated.[8]

These matrix methods, however, are not useful for real-time spectroscopy in solution at ambient temperature, where a spectroscopy-friendly nitrogen leaving-group precursor would be ideal. In 1965, Closs and Coyle reported that the chlorination of diazomethane with *tert*-butylhypochlorite at −100 °C gave monochlorodiazomethane, **2**, which thermally decomposed to chlorocarbene (CHCl) above −40 °C.[9] However, further chlorination of **2** at −100 °C led to rapid nitrogen loss. Although

† Rutgers, The State University of New Jersey.
‡ University of California.

(1) (a) Hine, J. *J. Am. Chem. Soc.* **1950**, *72*, 2438. (b) Hine, J.; Dowell, A.M., Jr. *J. Am. Chem. Soc.* **1954**, *76*, 2688. (c) Hine, J. *Divalent Carbon*; Ronald Press: New York, 1964; pp 36ff.
(2) Doering, W. v. E.; Hoffman, A. K. *J. Am. Chem. Soc*. **1954**, *76*, 6162.
(3) (a) Regitz, M., Ed. *Carbene, Carbenoide, Methoden der Organische Chemie (Houben-Weyl*); Thieme Verlag: Stuttgart, 1989; Vol. E19b. (b) Fedorynski, M. *Chem. Rev.* **2003**, *103*, 1099 and references therein.
(4) (a) Jones, M., Jr.; Sachs, W. H.; Kulczycki, A., Jr.; Waller, F. J. *J. Am. Chem. Soc*. **1966**, *88*, 3167. (b) Hartwig, J. F.; Jones, M., Jr.; Moss, R. A.; Lawrynowicz, W. *Tetrahedron Lett.* **1986**, *27*, 5907. (c) Presolski, S. I.; Zorba, A.; Thamattoor, D. M.; Tippmann, E. M.; Platz, M. S. *Tetrahedron Lett.* **2004**, *45*, 485.
(5) Chateauneuf. J. E.; Johnson, R. P.; Kirchoff, M. M. *J. Am. Chem. Soc.* **1990**, *112*, 3217.
(6) Milligan, D. E.; Jacox, M. E. *J. Chem. Phys.* **1967**, *47*, 703.
(7) Anastassiou, A. G.; Shepelavy, J. N.; Simmons, H. E.; Marsh, F. D. In *Nitrenes*; Lwowski, W., Ed.; Wiley-Interscience: New York, 1970; pp 305ff.
(8) Jacox, M. E.; Milligan, D. E. *J. Chem. Phys.* **1970**, *53*, 2688.
(9) Closs, G. L.; Coyle, J. J. *J. Am. Chem. Soc.* **1965**, *87*, 4270.

some dichlorodiazomethane (**3**) might have been produced under these conditions,[9] precursor **3** was obviously not useful as an ambient temperature source of CCl_2. Dichlorodiazirine (**4**) would likely be a more practical target. Although there are literature reports of the preparations of difluorodiazirine and chlorofluorodiazirine,[10] these involve dangerously explosive intermediates, and the methodology is not easily extended to the preparation of dichlorodiazirine.

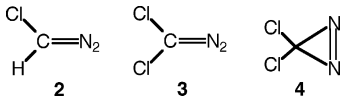

2 **3** **4**

Recently, we communicated the first synthesis of dichlorodiazirine, **4**, and showed that its thermal or photochemical decompositions at room temperature led to dichlorocarbene.[11] Here, we present full details of an improved preparation of **4**, as well as several LFP experiments involving CCl_2. N−, O−, and S−CCl_2 ylides or oxides have been identified in these experiments, and we also present results from electronic structure calculations on the ground and excited states of these species.

Results and Discussion

Preparation of Dichlorodiazirine, 4. Our approach to **4** is based on the diazirine exchange reaction, which permits the replacement of a leaving group of a halodiazirine by a nucleophile; cf. eq 2.[12] Diazirines **5**, with R = alkyl, aryl,

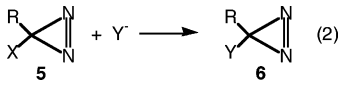

5 **6** (2)

alkoxy, or aryloxy, and X = Cl or Br, are readily available via the Graham oxidations of amidines or isouronium salts by hypochlorite or hypobromite.[13,14] Subsequent reaction of **5** with nucleophile Y^-, where Y = F, MeO, ArO, or CN, affords the new diazirines **6**.[12] In this way, a large variety of diazirines can be prepared as spectroscopy-friendly precursors for many carbenes. However, dihalodiazirines have not been available by this methodology.

In order to apply eq 2 to dihalodiazirine synthesis, the R group of **5** must be transformed into a leaving group. We accomplished this as follows: phenoxychlorodiazirine, **7**, readily available by oxidation[13] of the phenylisourea mesylate, **8**,[15] was nitrated with $NO_2^+BF_4^-$ (0 °C, $MeNO_2$), giving *p*-nitrophenoxychlorodiazirine, **9**.[16] The *p*-nitrophenoxy moiety of **9** represents a potential leaving group with a fugacity comparable to that of chloride.

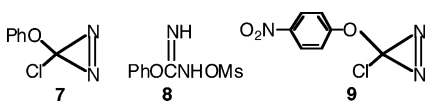

7 **8** **9**

Reaction of **9** with F^- follows three competitive pathways:[16] diazirine exchange reactions[12] lead either to fluorochlorodiazirine, **10** (by replacement of *p*-nitrophenoxide), or to *p*-nitrophenoxyfluorodiazirine, **11** (by replacement of chloride). At the same time, diazirinone **12** forms by *ipso* attack of F^- para to the nitro substituent of **9**.[16] Although the diazirinone-forming pathway dominates, the formation of **10** demonstrates the feasibility of dihalodiazirine synthesis by this methodology.

Reaction of **9** with a mixture of tetrabutylammonium chloride

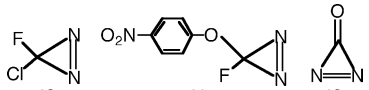

10 **11** **12**

(TBACl), CsCl, and the ionic liquid butylmethylimidazolium chloride (mp 55 °C) in a small volume of dry HMPA at 40−50 °C gives **4** in an analogous reaction; cf. eq 3. The yield of **4** does not exceed 20%, and the principal reaction product of **9** is probably diazirinone, formed by attack of chloride para to the nitro substituent. Nevertheless, this reaction constitutes the first synthesis of **4**.[11]

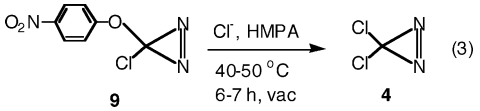

9 **4** (3)

However, the reaction described in eq 3 has proven to be less than satisfactory. Precursor **9** is not sufficiently reactive to chloride, and repetitive preparations are not always successful. We sought to improve the procedure for the preparation of **4**, and it is the improved procedure that we describe in detail here.

We find that 2,4-dinitrophenoxychlorodiazirine, **13**, is a better and more reliable progenitor of **4** than is its mononitrated relative **9**. Thus, 5 mmol of phenoxychlorodiazirine **7** in nitromethane is readily dinitrated by 15 mmol of $NO_2^+BF_4^-$ at 0 °C. A yield of about 75% of **13** can be purified and isolated by column chromatography over silica. Treatment of **13** with a 5:2:2 blend

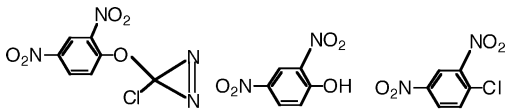

13 **14** **15**

of 1-butyl-3-methylimidazolium chloride, TBACl, and CsCl[17] in HMPA at 50 °C for 4 h gives **4**, which is removed under vacuum (∼0.1 mmHg) and trapped in pentane (or other solvent) at 77 K. Typically, from 250 mg of **13**, we obtain a 2-mL solution of **4** in pentane with a UV absorbance of 0.4 at 359 nm. The UV spectrum of **4** in pentane appears in Figure 1.

Halodiazirines typically absorb in the 350 nm region,[13] and **4** also displays an IR absorption at 1548 cm^{-1} which can be assigned to the N=N stretch.[13,18]

Optimization of the conditions indicated that the reaction temperature is important: if the temperature falls significantly below 50 °C, the reaction proceeds too slowly, whereas if the

(10) (a) Mitsch, R. A.; Neuvar, E. W.; Koshar, R. J.; Dybvig, D. H. *J. Heterocycl. Chem.* **1965**, *2*, 371. (b) Zollinger, J. L.; Wright, C. D.; McBrady, J. J.; Dybvig, D. H.; Fleming, F. A.; Kurhajec, G. A.; Mitsch, R. A.; Neuvar, E. W. *J. Org. Chem.* **1973**, *38*, 1065.
(11) Chu, G.; Moss, R. A.; Sauers, R. R. *J. Am. Chem. Soc.* **2005**, *127*, 14206.
(12) Moss, R. A. *Acc. Chem. Res.* **2006**, *39*, 267.
(13) Graham, W. H. *J. Am. Chem. Soc.* **1965**, *87*, 4396.
(14) Liu, M. T. H., Ed. *Chemistry of Diazirines*; CRC Press: Boca Raton, FL, 1987; Vols. I and II.
(15) Fedé, J.-M.; Jockusch, S.; Lin, N.; Moss, R. A.; Turro, N. J. *Org. Lett.* **2003**, *5*, 5027.
(16) Moss, R. A.; Chu, G.; Sauers, R. R. *J. Am. Chem. Soc.* **2005**, *127*, 2408.
(17) The chloride reagent mixture was preheated, dried, and liquified by heating to 80−85 °C under vacuum for 5 h.
(18) UV monitoring indicates that solutions of **4** are moderately stable in the dark at 25 °C: about 10% of decomposition occurs after 13 h.[11] The E_a for cleavage to $CCl_2 + N_2$ is calculated [B3LYP/6-311+G(2d)] at 28 kcal/mol.[11]

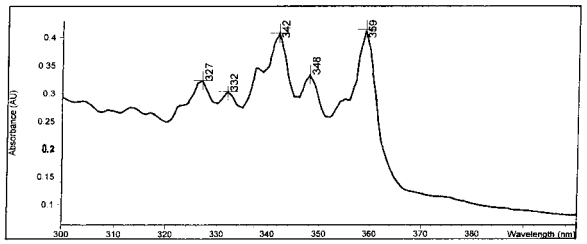

Figure 1. The UV spectrum of **4** in pentane; the darkness of the trace has been enhanced.

Scheme 1

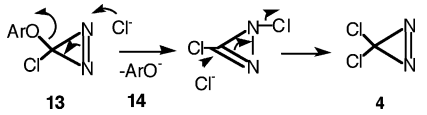

Scheme 2

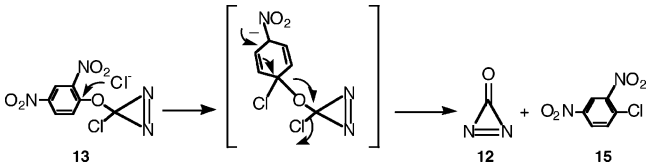

temperature exceeds 60 °C, the reaction solution turns red, the HMPA decomposes, and a byproduct forms with UV absorptions at 351, 362, and 374 nm. Variation of the chloride source showed that the use of either TBACl or butylmethylimidazolium chloride alone led to low yields of **4** and required longer reaction times (>8 h). The combination of butylmethylimidazolium chloride, TBACl, and CsCl gave the best yield of **4**, with the shortest reaction time, as described above.

Using our optimized conditions, GC analysis of the reaction residue revealed that 23% of 2,4-dinitrophenol (**14**) and 77% of 1-chloro-2,4-dinitrobenzene (**15**) remained after the generation of **4**. This implies that chloride attack on **13** occurred ~20% at diazirine N, leading to **4** and **14** via Scheme 1, and ~80% on the aromatic ring of **13**, leading to diazirinone and **15** via Scheme 2.

The diazirine exchange reaction of Scheme 1 is formulated with the normative double S_N2' attack mechanism,[12] where S_N2' attack of Cl^- at diazirine N leads to the loss of *p*-nitrophenoxide (subsequently protonated to **14**) and the generation of an isodiazirine. A second S_N2' chloride attack on the latter then affords **4**. Note that the alternative ejection of chloride in the initial S_N2' attack on **13** would simply lead back to **13** after the second S_N2' step. The competitive *ipso* attack on **13** is formulated, as in Scheme 2,[16] and leads to the formation of diazirinone and **15**. We did not verify the formation of diazirinone in this case. It is known that diazirinone fragments to nitrogen and carbon monoxide within ~5 min at ambient temperature.[16]

Generation and Reactions of Dichlorocarbene. Photolysis of **4** in tetramethylethylene (TME) or cyclohexene led to the expected CCl_2 adducts **16** and **17**. These products were identified by GC and GC−MS comparisons with authentic samples.

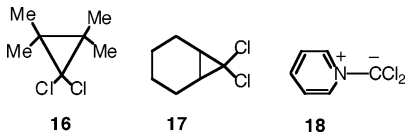

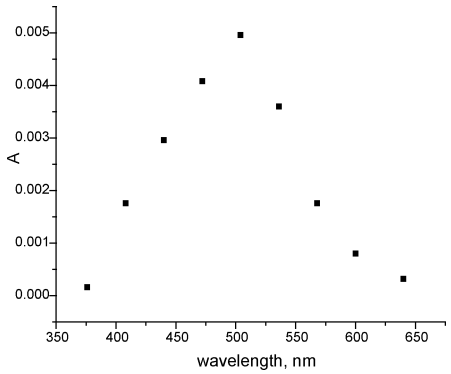

Figure 2. The UV spectrum of ylide **19** produced by LFP of **4** in the presence of 2-picoline.

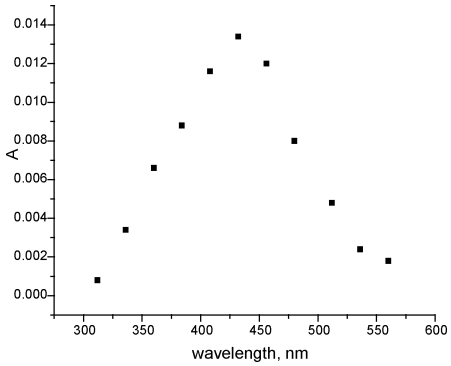

Figure 3. UV spectrum of ylide **21**, produced by LFP of **4** in the presence of thioanisole.

LFP of **4** in the presence of 0.4 M pyridine in pentane gave ylide **18**, identified by its UV absorption at 387 nm.[11] The same ylide (λ_{max} = 390 nm) was observed upon photoextrusion of CCl_2 from phenanthrene adduct **1**, followed by capture of the carbene by pyridine.[5] The UV spectrum of **18** has been published.[5,11] A similar UV spectrum was obtained when the CCl_2 was generated by photoextrusion from a CCl_2−indane adduct.[4c]

LFP generation of CCl_2 from **4** also led to ylide formation with 2-picoline; cf. ylide **19**, λ_{max} = 504 nm, Figure 2. However, no ylide (**20**) was generated upon LFP of **4** in the presence of 2,6-lutidine. Presumably, the two flanking methyl groups of the

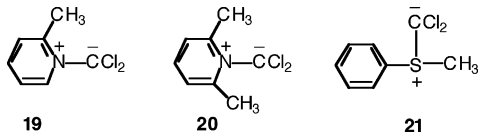

2,6-lutidine effectively shield the nitrogen from CCl_2 attack. Ylide formation was also observed when **4** was photolyzed with thioanisole. Here, capture of CCl_2 led to *S*-ylide **21**, λ_{max} = 432 nm; cf. Figure 3.

Computational Studies

These ylide-forming reactions were studied computationally. The computed energetics for the formation of singlet ylides **18**−**21** are shown in Table 1 (PBEPBE/6-311+G(d)).[19−21] The

(19) Perdew, J. P.; Burke, K.; Ernzerhof, M. *Phys. Rev. Lett.* **1996**, *77*, 3865.
(20) Krishnan, R.; Binkley, J. S.; Seeger, R.; Pople, J. A. *J. Chem. Phys.* **1980**, *72*, 650. McLean, A. D.; Chandler, G. S. *J. Chem. Phys.* **1980**, *72*, 5369. Clark, T.; Chandrasekhar, J.; Spitznagel, G. W.; Schleyer, P. v. R. *J. Comput. Chem.* **1983**, *4*, 294.

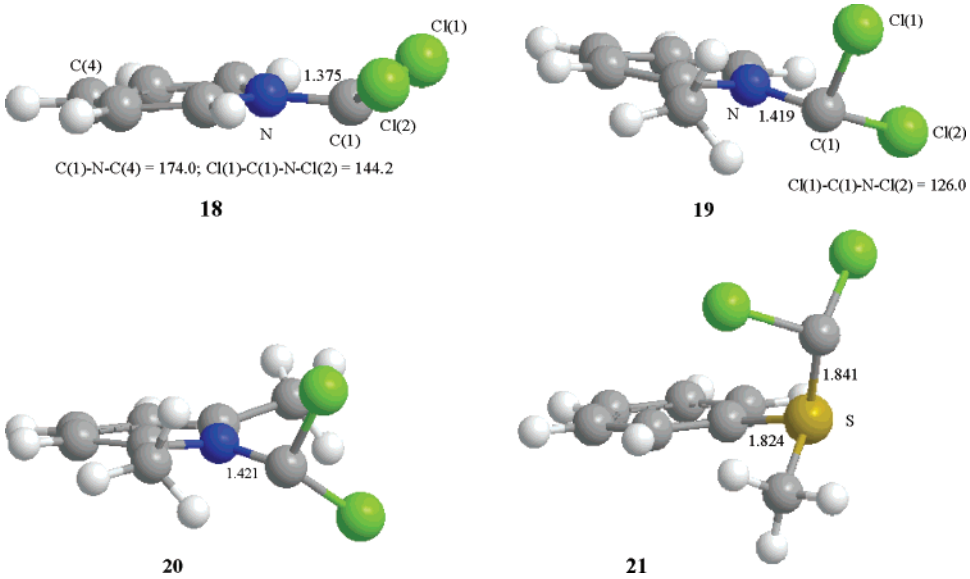

Figure 4. Structures of ylides **18**−**21** (PBEPBE/6-311+G(d)).

Table 1. Reaction Energies (kcal/mol) for Formation of Singlet Ylides **18**−**21**[a]

species	ΔE	ΔH	ΔG[b]
pyridine−CCl_2 ylide, **18**	−32.3	−30.0	−19.9
2-picoline−CCl_2 ylide, **19**	−27.9	−25.6	−13.8
2,6-lutidine−CCl_2 ylide, **20**	−21.0	−18.9	−5.8
thioanisole−CCl_2 ylide, **21**	−14.4	−12.9	−3.1

[a] Energies computed at PBEPBE/6-311+G(d) optimized geometries. [b] The free energies were computed using a reference state of 1 M concentration for each species participating in the reaction, and $T = 298.15$ K.

formation of sterically unhindered pyridine−CCl_2 ylide **18** is strongly exothermic ($\Delta H = -30.0$ kcal/mol).[22] Ylide **18** (C_s point group; symmetry plane bisecting the Cl−C(carbene)−Cl angle, Figure 4) has a short C(carbene)−N(pyridine) single bond length of 1.375 Å, and the C(carbene) atom is minimally displaced below the pyridine plane (<C(carbene)−N−C(para) = 174.0°). Slight pyramidalization occurs at C(carbene), and the Cl atoms are situated above the pyridine plane (<Cl(1)−C(carbene)−N−Cl(2) = 144.2°). The two electrons formally in the carbenic C(2p) orbital and the six pyridine π-electrons are well conjugated, forming an overall 8π-electron system.

To reduce steric interactions with the flanking methyl group in ylide **19**, the carbene unit has rotated around the N−C axis so that one Cl atom (Cl(2)) lies close to the pyridine plane opposite the methyl group and further pyramidalization occurs at the carbenic center (<Cl(1)−C(carbene)−N−Cl(2) = 126.0°, Figure 4). The angle between the formal lone-pair electrons on the carbenic center and the pyridine plane is approximately 55°, so π-electron conjugation is diminished in **19**. Relative to **18**, the C(carbene)−N(pyridine) bond length in **19** has increased by 0.04 Å to 1.419 Å, and the exothermicity for ylide formation is reduced slightly by about 4 kcal/mol ($\Delta H = -25.6$ kcal/mol). The difference between ΔH and ΔG for the formation of **19** is larger than that for the simpler ylide **18** (11.8 kcal/mol vs 10.1 kcal/mol), reflecting a modest increase in steric hindrance occurring in **19**.

With the addition of the second flanking methyl group in (computed) ylide **20**, the carbene unit is forced to occupy an orientation essentially perpendicular to the pyridine, which situates its lone-pair electrons almost in the pyridine plane. This sterically encumbered position (Figure 4) is reflected in an elongated C(carbene)−N(pyridine) bond length (1.421 Å) and a diminished exothermicity for ylide formation, $\Delta H = -18.9$ kcal/mol, about 7 kcal/mol greater than ΔH for the formation of **19**. The computed favorable reaction free energy ($\Delta G = -5.8$ kcal/mol) does of course not take account of the kinetic difficulty of forming **20**. The very limited number of successful trajectories to 2,6-lutidine, available to the carbene, suggests that there must be a very small and highly unfavorable pre-exponential factor in the rate expression, and therefore a very negative entropy of activation for the formation of **20**.

Whereas the carbene unit C atoms of ylides **18**−**20** lie essentially in the pyridine plane, σ-bonded to the lone pair on N through the C(p) orbital, the carbene unit C atom of *S*-ylide **21** is situated well above the ring plane with both the S and C(carbene) atoms adopting a pseudotetrahedral configuration (the fourth site is occupied by a lone pair in each case); cf. Figure 4. The S−C(carbene) bond length is 1.841 Å, only slightly longer than the S−C(phenyl) bond length (1.824 Å). The Cl atoms are oriented toward the ring, straddling the C−S bond, and the lone pair on C is thus pointing away from the phenyl π-system. Not surprisingly, the reaction enthalpy of formation for **21**, $\Delta H = -12.9$ kcal/mol (Table 1), is less than those computed for the *N*-ylides **18**−**20**. Although the free energy of formation of **21** is computed to be only slightly favorable ($\Delta G = -3.1$ kcal/mol), there is minimal steric hindrance opposing CCl_2 addition to thioanisole and the formation of ylide **21** is not kinetically prohibited.[23] We also note earlier, important experimental studies of sulfide−CCl_2

(21) Frisch, M. J.; et al. *Gaussian 03*, revision B.03; Gaussian, Inc.: Pittsburgh, PA, 2003. See Supporting Information for the complete reference to Gaussian 03.

(22) Pliego, R. J., Jr.; De Almeida, W. B. *Phys. Chem. Chem. Phys.* **1999**, *1*, 1031 report an exothermicity of $\Delta H = -35.5$ kcal/mol for this reaction on the basis of MP4/6-311G(2df,p)//MP2/6-31G* calculations.

(23) We also located two π-type CCl_2−thioanisole complexes, which are analogous to the CCl_2−anisole complexes investigated previously by computational means by us (Krogh-Jespersen, K.; Yan, S.; Moss, R. A. *J. Am. Chem. Soc.* **1999**, *121*, 6269). However, these π-type CCl_2−thioanisole complexes were found to be 7−8 kcal/mol higher in energy than ylide **21** and, hence, are not energetically competitive.

Table 2. Computed (TD-PBEPBE/6-311+G(d)) Absorption Wavelengths (λ, nm) and Oscillator Strengths (f) for the Two Singlet−Singlet Transitions of Lowest Energy in Ylides **18**, **19**, **21**, and **22**[a]

species	medium	λ_1	f_1	λ_2	f_2	λ_{exp}[b]
pyridine−CCl_2 ylide, **18**	vacuum	424.8	0.013	382.7	0.167	
pyridine−CCl_2 ylide, **18**	heptane	427.1	0.013	394.9	0.229	387
2-picoline−CCl_2 ylide, **19**	vacuum	473.9	0.026	451.0	0.154	
2-picoline−CCl_2 ylide, **19**	heptane	473.2	0.115	455.8	0.058	504
thioanisole−CCl_2 ylide, **21**	vacuum	450.9	0.088	424.7	0.007	
thioanisole−CCl_2 ylide, **21**	heptane	439.2	0.097	397.6	0.004	432
CCl_2-carbonyl oxide, **22S**	vacuum	499.8	0.0001	344.3	0.031	
CCl_2-carbonyl oxide, **22S**	heptane	478.5	0.0001	334.5	0.036	465
CCl_2-carbonyl oxide, **22T**	vacuum	493.8	0.0004	451.6	0.004	
CCl_2-carbonyl oxide, **22T**	heptane	478.8	0.0006	466.7	0.004	465

[a] Computational data are presented for (a) idealized gas-phase conditions (vacuum) and (b) simulated experimental conditions (CPCM solvation model, heptane) to represent the solvent used experimentally (pentane).[b] This work; solvent is pentane.

ylides. However, these did not involve dichlorodiazirine or spectroscopic characterization.[24]

We have also investigated the electronic structures of ylides **18**−**21** with the 6-311+G(d) basis set and the B3LYP[25] (rather than PBEPBE) exchange and correlation functionals. As expected, the molecular geometries of **18**−**21** produced by the two sets of functionals are very similar (Supporting Information). However, the reaction energies for ylide formation are 6−8 kcal/mol less favorable with the B3LYP functionals (Supporting Information, Table S-1).

Energies of the low-lying excited singlet states of ylides **18**, **19**, and **21** were computed at the optimized ground-state geometries at the TD-PBEPBE/6-311+G(d) level,[26] and the predicted (vertical) absorption wavelengths and oscillator strengths are collected in Table 2. Computational data are presented for idealized gas-phase conditions (vacuum) and simulated experimental conditions where we employed the CPCM polarizable conductor solvation model[27] and heptane parameters to represent the solvent used experimentally (pentane). The experimentally well-characterized absorption band near 390 nm for ylide **18** actually consists of two electronic transitions carrying very different intensities. Both transitions are charge-transfer in nature, originating in the C(carbene) lone pair of π-symmetry and terminating in the two low-lying pyridine unoccupied MOs (the two-fold degeneracy of the π*-LUMOs in benzene is broken slightly in pyridine). The transition to the unoccupied MO, which has a significant atomic orbital contribution from the N atom, carries considerably more intensity than the transition terminating in the MO having a node on the N atom ($f \approx 0.23$ for the stronger component vs $f \approx 0.01$ for the weaker component). The numerical agreement between the computed absorption wavelength of 394.9 nm and the experimental observation is excellent.

Due to the rotation of the carbene unit in ylide **19**, the interaction between the C(carbene) and the pyridine π-systems is reduced, relative to those for ylide **18**. Consequently, the electronic absorption band in **19**, λ_{max}(exp) = 504 nm, is considerably red-shifted relative to that of **18**. The computed

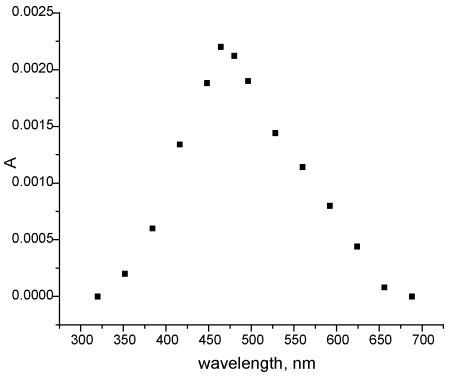

Figure 5. Transient UV spectrum observed upon LFP of **4** in pentane.

major component transition has λ = 473.2 nm but is reduced in intensity ($f \approx 0.12$), relative to that of **18**, due to the diminished carbene−pyridine π-overlap. The minor component transition is predicted to be slightly higher in energy (λ = 455.8 nm, $f \approx 0.08$), thus contributing to the substantial broadness of the observed band (viz. Figure 2). (Calculations predict a further red-shift in the electronic absorption band to λ = 536 nm ($f \approx 0.14$) in putative ylide **20**.)

For ylide **21**, the electronic transitions of lowest energy occur from the carbene lone pair into the phenyl π*-orbitals. The computed wavelength for the component carrying major intensity, λ = 439.2 nm ($f \approx 0.10$), is in very good agreement with the experimentally observed λ_{max} = 432 nm.

We have also evaluated the electronic transition energies for ylides **18**−**21** using TD-B3LYP/6-311+G(d) methodology (at the B3LYP/6-311+G(d) geometries). The overall spectroscopic pattern (number of low-lying transitions as well as their relative energies and intensities) matches closely that described above obtained with the PBEPBE functionals; however, the computed transition energies are uniformly higher and, except for the case of **18**, exceed the experimentally observed peaks (typically by a few tenths of an eV; Supporting Information, Table S-2). The higher B3LYP transition energies are presumably principally due to the presence of (exact) Hartree−Fock exchange in the B3 functional[25] and are not a result of differences in the B3LYP vs PBEPBE optimized molecular geometries. (TD-B3LYP/6-311+G(d) calculations on PBEPBE/6-311+G(d) optimized geometries also predict transition energies larger than the experimental values.)

Reaction of CCl_2 with Oxygen. LFP of **4** in pentane at 25 °C affords the UV spectrum shown in Figure 5. The observed transient displays λ_{max} = 465 nm and exhibits a lifetime of ~0.5 μs, $k_{decay} = 2.2 \times 10^6$ s^{-1}. Previously, we tentatively assigned its identity as CCl_2.[11] Its absorbance also agrees with the Milligan−Jacox report of 460−530 nm, assigned to matrix-isolated CCl_2.[6,8] The computed $\sigma \rightarrow$ p transition of CCl_2 in simulated heptane occurs at λ = 491.9 nm ($f \approx 0.004$; and λ = 486.4 nm, $f \approx 0.004$ in vacuum; TD-PBEPBE/6-311+G(d)).

Unfortunately, the transient of Figure 5 cannot be CCl_2: it is *not* quenched by TME, which is known to quench CCl_2 with $k_q = 3.8 \times 10^9$ M^{-1} s^{-1}.[5,28,29] Even more persuasive is our

(24) Parham, W. E.; Groen, S. H. *J. Org. Chem.* **1964**, *29*, 2214; **1965**, *30*, 728; **1966**, *31*, 1694.
(25) Becke, A. D. *J. Chem. Phys.* **1993**, *98*, 5648. Lee, C.; Yang, W.; Parr, R. G. *Phys. Rev. B* **1988**, *37*, 785.
(26) Casida, M. E.; Jamorski, C.; Casida, K. C.; Salahub, D. R. *J. Chem. Phys.* **1998**, *108*, 4439.
(27) Barone, V.; Cossi, M. *J. Phys. Chem. A* **1998**, *102*, 1995.
(28) We repeated the determination of k_q for the TME/CCl_2 reaction using CCl_2 generated from **4** by LFP, monitoring the reaction via the pyridine ylide method.[29] We obtained $k_q = 2.6 \times 10^9$ M^{-1} s^{-1}, in good agreement with the literature value[5] obtained with CCl_2 extruded from **1** by LFP.
(29) Jackson, J. E.; Soundararajan, N.; Platz, M. S.; Liu, M. T. H. *J. Am. Chem. Soc.* **1988**, *110*, 5595.

finding that the transient of Figure 5 is *only* observed when the LFP of **4** is carried out under a normal atmosphere containing oxygen. Repetition of the LFP experiment under nitrogen, with a thoroughly degassed **4**-pentane solution, afforded *no* transient absorbing in the 300−700 nm spectral region.

In view of these results, we suggest that a possible alternative for the 465 nm transient of Figure 5 might be carbonyl oxide **22**, formed by the reaction of CCl_2 with oxygen. A potential problem with assigning **22** as the transient of Figure 5 is that singlet carbonyl oxide formation by the reaction of a carbene with oxygen is usually expected from triplet carbenes, where the triplet carbene plus triplet oxygen combination is a spin-allowed process. For example, the reaction of ground-state triplet diphenylcarbene with $^3O_2$ to give singlet **23** is fast, with $k = (1 - 5) \times 10^9$ M^{-1} s^{-1}.[30] The reaction of a singlet carbene such as CCl_2 with $^3O_2$ to form a carbonyl oxide, however, is formally "spin-forbidden" and could be slow. Nevertheless, reactions of singlet carbenes with O_2 to furnish carbonyl oxides are known; for example, phenylchlorocarbene (PhCCl) reacts with oxygen to form singlet oxide **24** with $k = 1.2 \times 10^6$ M^{-1} s^{-1} in Freon 113 at room temperature.[31] The same reaction even occurs in an argon matrix at 35 K.[32] Sawaki et al. suggest that $^3O_2$ reacts with *triplet* PhCCl present in a thermally driven singlet−triplet PhCCl equilibrium They estimate that the ^{1}PhCCl/^{3}PhCCl differential free energy is ∼4 kcal/mol.[31] Sheridan et al. suggested that complexation between ^{1}PhCCl and $^3O_2$ (in the matrix) could facilitate intersystem crossing to ^{3}PhCCl prior to reaction with $^3O_2$.[32]

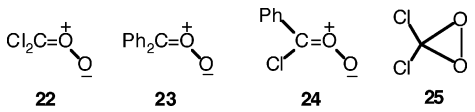

22 **23** **24** **25**

The singlet−triplet energy separation for CCl_2 is computed at ∼19 kcal/mol,[33] however, making analogous mechanisms very unlikely for the reaction between CCl_2 and O_2. Furthermore, the lowest excited singlet state of O_2 is also approximately 20 kcal/mol above the triplet ground state.[34] Thus, under ambient conditions, the spin-allowed formation of **22** by direct reaction between $^1CCl_2$ and a thermally excited $^1O_2$, or between a thermally excited $^3CCl_2$ species and $^3O_2$, does not seem plausible. On the other hand, persuasive arguments based on data from electronic structure calculations on the $CCl_2 + O_2$ system can be offered in support of the formation of both singlet and triplet **22** from the reaction of $^1CCl_2$ and $^3O_2$.

Scans of the singlet and triplet potential energy surfaces for $CCl_2 + O_2$ at the PBEPBE/6-311+G(d) level revealed several stationary points. A triplet carbonyl oxide minimum of C_s symmetry, **22T**, with $\Delta G = -7.0$ kcal/mol (Table 3), relative to separated $^1CCl_2$ and $^3O_2$, can form in a spatial- and spin-symmetry allowed reaction, without an apparent activation energy.[35] In **22T**, O(1)−O(2) adopts a bisected orientation with respect to the CCl_2 plane, and the C atom is slightly pyramidalized; the pyramidalization at C is such that the O(2) and Cl atoms are on the same side of the C−O(1) bond.[36] The unpaired electrons are principally located on the terminal O(2) atom ($\rho = 0.86$) and on the C atom ($\rho = 0.70$), in perpendicularly oriented 2p orbitals. The C−O(1) and O(1)−O(2) bond lengths are 1.371 and 1.387 Å, respectively, indicative of single bonds.

Table 3. Energies (kcal/mol) of Cl_2CO_2 Species, Relative to Separated $^1CCl_2$ and $^3O_2$[a]

species	ΔE	ΔH	ΔG[b]
$^1CCl_2 + {}^3O_2$	0.0	0.0	0.0
CCl_2-carbonyl oxide, triplet, **22T**	−16.2	−15.1	−7.0
CCl_2-carbonyl oxide, singlet, **22S**	−44.7	−42.4	−33.0
dichlorodioxirane, singlet, **25**	−65.6	−63.4	−53.6
TS, **22S**−**25**[c]	−25.2	−24.1	−14.3

[a] Energies computed at PBEPBE/6-311+G(d) optimized geometries. [b] The free energies were computed using a reference state of 1 M concentration for each species participating in the reaction, and $T = 298.15$ K. [c] Singlet state.

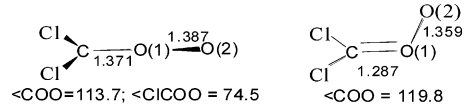

Singlet carbonyl oxide, **22S**, is planar with a C−O(1) distance of 1.287 Å, and the O(1)−O(2) bond length is 1.359 Å, suggesting a resonance structure $Cl_2C{=}O^+{-}O^-$ with a "double" C−O and a "single" O−O bond. The triplet−singlet free energy separation in **22** is −26.0 kcal/mol (Table 3). Dichlorodioxirane, **25**, represents another minimum on the singlet potential energy surface, 20.6 kcal/mol below **22S** in free energy. A nonplanar transition state interconnects **22S** and **25**. Due to the large structural and bonding differences between **22S** and **25**, there is a substantial barrier for the isomerization, $\Delta G^{\ddagger} = 18.7$ kcal/mol relative to **22S**.

Importantly, TD-PBEPBE/6-311+G(d) excited-state calculations predict low-energy electronic transitions for **22** near 475 nm in simulated heptane (Table 2) which is a good match for the observed absorption maximum in Figure 5. The calculations indicate that **22S** and/or **22T** could be responsible for the observed absorption. The calculations for **22S** predict one singlet−singlet absorption in the desired spectral region at 478.5 nm, although the predicted intensity is very weak ($f \approx 0.0001$). The nature of this transition provides a rationalization for the computed weakness. Examination of eigenvectors shows that this transition may be characterized as a very pure $n_{O(2)}-\pi_{CO(1)}^*$ electronic excitation, arising from an in-plane 2p lone-pair on O(2) and terminating in a (perpendicularly oriented) π^* orbital, which is almost exclusively concentrated on C and O(1).[37] The calculations for **22T** predict several triplet−triplet transitions in the 350−500 nm range, including absorptions at 478.8 nm ($f \approx 0.0006$) and 466.7 nm ($f \approx 0.004$).[38] Additional calculations

(30) (a) Closs, G. L.; Rabinow, B. E. *J. Am. Chem. Soc.* **1976**, *98*, 8190. (b) Werstiuk, N. H.; Casal, H. L.; Scaiano, J. C. *Can. J. Chem.* **1984**, *62*, 2391.
(31) Makihara, T.; Nojima, T.; Ishiguro, K.; Sawaki, Y. *Tetrahedron Lett.* **2003**, *44*, 865.
(32) Ganzer, G. A.; Sheridan, R. S.; Liu, M. T. H. *J. Am. Chem. Soc.* **1986**, *108*, 1517.
(33) Barden, C. J.; Schaefer, H. F., III. *J. Chem. Phys.* **2000**, *112*, 6515.
(34) Schweitzer, C.; Schmidt, R. *Chem. Rev.* **2003**, *103*, 1685.

(35) A weakly bound complex ($\Delta E = -0.5$ kcal/mol, $\Delta H = +0.4$ kcal/mol, and $\Delta G = 3.9$ kcal/mol), formed between unperturbed $^1CCl_2$ and $^3O_2$ with a $Cl_2C{\cdots}OO$ distance of about 3 Å, was located at the B3LYP/6-31g(d) level. Similarly, at this computational level, a transition state ($\Delta E^{\ddagger} = 2.5$ kcal/mol, $\Delta H^{\ddagger} = 2.8$ kcal/mol, and $\Delta G^{\ddagger} = 11.8$ kcal/mol) with a $Cl_2C{\cdot\cdot}{\cdot}OO$ distance of about 2.0 Å leads from the weakly bound complex to the triplet carbonyl oxide. These stationary points are not present when the PBEPBE functionals are applied in the calculations. See the Supporting Information for additional structural and energetic details.
(36) A second triplet conformer, in which the pyramidalization at C is opposite, has a relative free energy 1.6 kcal/mol higher; the activation free energy barrier is 2.3 kcal/mol relative to that of **22T**.
(37) The transition computed in **22S** is thus analogous to the weak $n-\pi^*$ absorptions exhibited by simple aldehydes and ketones.

predict that the lowest-energy transition of dichlorodioxirane **25** should appear at 377 nm ($f \approx 0.0008$).

The calculations predict that singlet **22S** should encounter a significant barrier to ring closure and could absorb in the desired UV region, but how efficiently can it be formed from triplet **22T**? To answer this question, we have carried out CASSCF-(6,6)/6-311+G(d) calculations on **22S** and **22T**, and have located the minimum-energy crossing point (conical intersection) between the triplet and singlet potential energy surfaces.[39] According to these CASSCF calculations, the **22S**−**22T** electronic energy separation is 16.2 kcal/mol, and a crossing point, i.e., a molecular geometry where **22T** and **22S** are isoenergetic, is located only 1.8 kcal/mol above the **22T** minimum. The crossing point shows a change in the ClCOO dihedral angle of approximately 23° away from the perpendicular orientation in **22T** toward planarity (**22S**). The magnitude of the spin−orbit coupling between the two electronic states is 10.4 cm^{-1} at the crossing point.

Thus, three factors combine to indicate that the triplet-to-singlet intersystem crossing (ISC) of **22T** to **22S** should be facile: (1) the activation energy is very small, (1.8 kcal/mol ≈ $3RT$, $T = 298$ K); (2) the geometry of the crossing point is very similar to the equilibrium geometry for **22T**, hence, easily accessible at ambient temperature; and (3) the magnitude of the spin−orbit coupling (10.4 cm^{-1}) is not insignificant, reflecting the presence of two "heavy" Cl atoms in the molecule.

A numerical estimate of the rate constant for ISC in **22** can be obtained by application of "Fermi's Golden Rule" to radiationless transitions.[40,41] In the high-temperature limit, the rate constant expression takes the form:

$$k_{ISC} = (4\pi^2/h)|H_{SO}|^2 \,\mathrm{FCWD} \qquad (4)$$

Here $|H_{SO}|$ is the magnitude of the spin−orbit coupling vector, and FCWD is the Franck−Condon weighted density of vibrational states (h = Planck's constant). FCWD may be expressed in terms of the exothermicity of the reaction (ΔE) and the reorganization energy (λ)

$$\mathrm{FCWD} = (4\pi\lambda RT)^{-1/2} \exp\left(-\left[\frac{(\Delta E + \lambda)^2}{(4\lambda RT)}\right]\right) \qquad (5)$$

If we ignore solvation energy differences, we may approximate λ by the difference in triplet energies for **22** evaluated at the triplet and singlet equilibrium geometries, respectively.[42] Using CASSCF derived energies ($\Delta E = -16.2$ kcal/mol, $H_{SO} = 10.4$ cm^{-1}, $\lambda = 27.7$ kcal/mol), we obtain $k_{ISC} \approx 3.5 \times 10^9$ s^{-1} at $T = 298$ K, thus confirming the qualitative analysis presented above.[43] The formation of **22S** from reaction of $^1CCl_2$ and $^3O_2$ should be very rapid at ambient conditions.

On the basis of the experimental results and the computational studies, we suggest the following (speculative) scenario for the experimental result presented in Figure 5. LFP of **4** under air generates CCl_2, which is captured by oxygen, affording triplet CCl_2-carbonyl oxide **22T**. The latter undergoes ISC to singlet **22S**. Both of these processes are extremely rapid, with rate constants in the 10^9 regime, and both are substantially exothermic. CCl_2-carbonyl oxide **22S**, which faces a significant barrier to cyclization to dioxirane **25**, is relatively long-lived ($\tau \approx 4-5$ μs), and is currently the best candidate for the observed UV band at 465 nm.[44]

Summary

Dichlorodiazirine (**4**) can be prepared by the reaction of 2,4-dinitrophenoxychlorodiazirine (**13**) and chloride. Photolysis of dichlorodiazirine generates dichlorocarbene which, in LFP experiments, forms chromophoric ylides or oxides with pyridine, 2-picoline, thioanisole, and oxygen. These species are readily observable by UV absorption spectroscopy. However, with the assignment of the 465 nm absorption from the LFP-UV of **4** under air to carbonyl oxide **22**, we can find no absorption attributable to CCl_2 itself, certainly not the $\sigma \rightarrow$ p absorption computed near 500 nm. Perhaps the CCl_2 absorption is simply too weak to be detected under our current conditions, in which case it is not surprising that CCl_2 absorbance was not found in LFP experiments with precursor **1**, especially in light of the interference from triplet phenanthrene.[5] It would certainly be of interest to study the low-temperature photolysis of matrix-isolated **4**, where higher concentrations of CCl_2 could perhaps be obtained.

Experimental Section

2,4-Dinitrophenoxychlorodiazirine (13). A solution of 0.85 g (5 mmol) of phenoxychlorodiazirine (**7**)[15] in 10 mL of nitromethane was added dropwise over 10 min into a magnetically stirred suspension of 2.0 g (15 mmol) of nitronium tetrafluoroborate in 10 mL of nitromethane at 0 °C. After the addition, the reaction mixture was stirred at 0 °C for 2 h until the reaction was complete (as monitored by TLC). Then, 200 mL of water was added, and the resulting solution was extracted with 5 × 50 mL of pentane. The pentane extract was dried over $MgSO_4$, filtered, concentrated on the rotary evaporator, and chromatographed over a silica column using 1:5 ether/pentane as eluent. We obtained 0.95 g (75%) of **13** as pale-yellow oil, which solidified at −20 °C in the freezer. **CAUTION**: All diazirines should be regarded as explosive. Work should be carried out behind safety shields, and in general, the diazirines should not be handled neat. It is best to store **13** as a solution in ether or pentane in the freezer.

^{1}H NMR (400 MHz, δ, $CDCl_3$): 8.09−8.12 (d, 1H, $J = 9.2$ Hz), 8.62−8.64 (d, 1H, $J = 9.2$ Hz), 8.84 (s, 1H). ^{13}C NMR (100 MHz, δ, $CDCl_3$): 68.82, 118.78, 121.48, 122.56, 125.97, 129.12, 149.29.

Dichlorodiazirine (4). A 25-mL flask with a tall neck bearing a side exit tube and containing a magnetic stirring bar was charged with 0.87 g (5.0 mmol) of anhydrous 1-butyl-3-methylimidazolium chloride, 0.56 g (2.0 mmol) of TBACl, and 0.34 g (2.0 mmol) of CsCl. The exit tube was connected to a series of two traps; the first was cooled to −20 °C, and the second, containing 1 mL of pentane, benzene, or other solvent, was cooled to 77 K. The second trap was fitted with stopcocks at both its inlet and outlet.

(38) Additional excitations are computed at 425.2 nm ($f \approx 0.0003$) and at 356.2 nm ($f \approx 0.005$). A near-infrared transition with no intensity is also predicted at $\lambda = 1217$ nm ($f = 0.0000$)

(39) Bearpark, M. J.; Robb, M. A.; Schlegel, H. B. *Chem. Phys. Lett.* **1994**, *223*, 269.

(40) Loudon, R. *The Quantum Theory of Light*; Oxford University Press: Oxford, 1983.

(41) Newton, M. *Chem. Rev.* **1987**, *87*, 113. Marcus, R. A. *Rev. Mod. Phys.* **1993**, *65*, 599.

(42) Beljonne, D.; Shuai, Z.; Pourtois, G.; Bredas, J. L. *J. Phys. Chem. A* **2001**, *103*, 3899.

(43) Using PBEPBE/6-311+g(d) derived energies ($\Delta E = -28.4$ kcal/mol, $\lambda =$ 23.0 kcal/mol) and $H_{SO} = 10.4$ cm^{-1}, we obtain $k_{ISC} \approx 3.1 \times 10^9$ s^{-1} at $T = 298$ K.

(44) This assignment should still be regarded as provisional. Although the 465 nm absorption clearly results from the reaction of CCl_2 with oxygen, and computational studies provide for an extremely rapid formation of **22**, we are unable to quench the absorbing species with TME, acetaldehyde, or tris(trimethylsilyl)silane, nor do we observe the formation of other UV active species (over 10 μs) as the 465 nm species decays.

The chloride mixture in the reaction flask was warmed to 80−85 °C under vacuum for 5 h to ensure dryness. During this time, the mixture melted and became homogeneous. It was then cooled to 50 °C. Next, 0.25 g (1.0 mmol) of 2,4-dinitrophenoxychlorodiazirine in 2 mL of anhydrous HMPA (dried over 13X molecular sieves) was slowly added to the reaction vessel via an addition funnel. During the addition, the reaction temperature was maintained at 50 °C and the vacuum at 0.1 mmHg. When the diazirine was added, effervescence was observed in the reaction mixture. After the addition was complete, the vacuum was maintained until the effervescence ceased (∼4 h). The outlet stopcock of the second trap (to the vacuum pump) was then closed, and nitrogen was admitted to the reaction train via the addition funnel until the systemic pressure reached 1 atm. The inlet stopcock of the second trap (now containing a solution of dichlorodiazirine) was closed, and the trap was removed. An additional 1 mL of solvent was added to the second trap, and its contents were transferred to a small storage flask while still cold (<−20 °C). We thus obtained a solution of **4** in 2 mL of (e.g.) pentane with $A_{359} = 0.4$. The UV spectrum of **4** appears in Figure 1.

Irradiation of this solution (Rayonet reactor, 350 nm) with 0.2 mL of added tetramethylethylene or cyclohexene for 1 h at 25 °C gave the known dichlorocarbene adducts of these alkenes. The adducts were identified by GC and GC−MS comparisons with authentic samples prepared by phase-transfer catalyzed additions of CCl_2 to the alkenes ($CHCl_3$ + 50% aqueous NaOH).

Laser Flash Photolysis. The LFP installation used a Lambda Physik EMG 101 excimer laser operating at 351 nm (XeF_2) and emitting 14-ns light pulses. The detection system featured an Applied Photophysics #720 150 W pulsed xenon lamp with an ARC 620 lamp igniter, and an ARC 0-3-102 lamp pulser, a 1-in. Uniblitz shutter and a Uniblitz 100-2B shutter drive control, an Instruments SA grating monochromator, and an RCA 4840 photomultiplier tube wired in a 5-dynode configuration. Data collection and analysis utilized a Stanford Research Systems DG535 four-channel digital delay/pulse generator and a Tektronix TDA 520A two-channel digitalizing oscilloscope. Data analysis used the Igor Pro 4.01 program (Wave Metrics, Inc.).

Electronic Structure Calculations. Electronic structure calculations were carried out with the Gaussian 03 suite[21] of programs. Geometry optimizations were carried out using density functional theory and PBEPBE[19] or B3LYP[25] exchange-correlation functionals with 6-311+g-(d) basis sets[20] (PBEPBE/6-311+G(d) and B3LYP/6-311+G(d)). Stationary points were characterized further by normal-mode analysis. The (unscaled) vibrational frequencies formed the basis for the calculation of vibrational zero-point energy (ZPE) corrections. Standard thermodynamic corrections (based on the harmonic oscillator/rigid rotor approximations and ideal gas behavior) were made to convert from purely electronic reaction or activation energies (ΔE, $\Delta E^{\ddagger}$no ΔZPE) to (standard) enthalpies (ΔH, $\Delta H^{\ddagger}$; ΔZPE included) and free energies (ΔG, $\Delta G^{\ddagger}$; $T = 298.15$ K, $P = 1$ atm).[45] The free energies presented in Tables 1 and 3 were computed using a reference state of 1 M concentration for each species participating in the reaction, and $T = 298.15$ K.

Excited-state calculations (transition energies (λ) and oscillator strengths (f)) at the optimized ground-state geometries used time-dependent density functional theory[25] and these same functional/basis set combinations (TD-PBEPBE/6-311+G(d)//PBEPBE/6-311+G(d) and TD-B3LYP/6-311+G(d)//B3LYP/6-311+G(d)). General solvent effects were incorporated in the excited-state calculations through application of the CPCM self-consistent reaction field model,[27] using default heptane parameters provided in Gaussian 03 to simulate the pentane solvent used experimentally.

Finally, CASSCF(6,6)/6-311+G(d) calculations were carried out on the two spin states of carbonyl oxide **22**, and the minimum-energy crossing point between the two surfaces was located.[39]

Acknowledgment. We are grateful to the National Science Foundation for financial support.

Supporting Information Available: Complete ref 21; optimized geometries and energies for ylides **18**−**21** (PBEPBE/6-311+G(d) and B3LYP/6-311+G(d); reaction and electronic transition energies at the B3LYP/6-311+g(d) level for **18**−**21**; optimized geometries and energies for the CCl_2 + O_2 species **22** (PBEPBE/6-311+G(d), B3LYP/6-31G(d), and CASSCF-(6,6)/6-311+G(d)). This material is available free of charge via the Internet at http://pubs.acs.org.

JA068727W

(45) McQuarrie, D. A. *Statistical Thermodynamics*; Harper and Row: New York, 1973.